

Research paper

Enhanced *in vitro* permeation of furosemide loaded into thermally carbonized mesoporous silicon (TCPSi) microparticlesAnn Marie Kaukonen ^{a,*}, Leena Laitinen ^a, Jarno Salonen ^c, Jaani Tuura ^c,
Teemu Heikkilä ^c, Tarja Linnell ^{a,b}, Jouni Hirvonen ^b, Vesa-Pekka Lehto ^c^a Drug Discovery and Development Technology Center, University of Helsinki, Finland^b Division of Pharmaceutical Technology, University of Helsinki, Finland^c Department of Physics, University of Turku, Turku, Finland

Received 12 July 2006; accepted in revised form 24 November 2006

Available online 1 December 2006

Abstract

The combined release and permeation behavior of furosemide loaded into thermally carbonized mesoporous silicon (TCPSi) microparticles was studied in order to evaluate the potential of TCPSi-loading to improve permeation of furosemide, a BCS class IV compound. Permeation was studied across Caco-2 monolayers at pH 5.5, 6.8 and 7.4 from drug solutions and TCPSi particles. TCPSi-loaded furosemide (39% w/w) exhibited improved dissolution from the microparticles with greatly diminished pH dependence. At pH 5.5, where furosemide solubility restricted the amount that could be dissolved in the control solution to less than 30% of the dose contained in the TCPSi particles, the flux of TCPSi-loaded furosemide across Caco-2 monolayers was over fivefold compared to pre-dissolved furosemide. The improved permeation could be confirmed also from dose-corrected (% dose-permeated) results. At pH 6.8 and pH 7.4, where corresponding doses could be used in control solutions, more than fourfold permeability values were obtained with TCPSi-loaded furosemide. Effects on transepithelial electrical resistance (TEER) and mannitol permeability were monitored and suggest that monolayer integrity was not compromised by the drug-loaded TCPSi microparticles. The improved permeation observed from furosemide-loaded TCPSi particles suggests that the high local concentrations provided by the enhanced dissolution properties of TCPSi-loaded furosemide could prove beneficial for absorption.

© 2006 Elsevier B.V. All rights reserved.

Keywords: Porous silicon; Microparticles; Dissolution; Permeation; Thermally carbonized silicon; Non-erosive drug matrix; Poorly soluble compounds

Abbreviations: BCS, biopharmaceutical classification system; C_0 , initial concentration ($\mu\text{g/ml}$); DMSO, dimethylsulfoxide; DSC, differential scanning calorimetry; FBS, fetal bovine serum; FTIR, Fourier transform infrared (spectroscopy); GI, gastro-intestinal; HBSS, Hanks' balanced salt solution; HF, hydrofluoric acid; HF:EtOH, hydrofluoric acid:ethanol; DMEM, Dulbecco's modified Eagle's medium; HPLC, high-performance liquid chromatography; $\log P$, octanol–water partitioning coefficient; NEAA, non-essential amino acids; P_{app} , apparent permeability coefficients (cm/s); pK_a , ionization constant; TCPSi, thermally carbonized mesoporous silicon (microparticles); TEER, transepithelial electrical resistance; TG, thermogravimetry.

* Corresponding author. Faculty of Pharmacy, Drug Discovery and Development Technology Center, P.O. Box 56 (Viikinkaari 5 E), FI-00014 University of Helsinki, Finland. Tel.: +358 9 191 59 736; fax: +358 9 191 59 144.

E-mail address: ann.m.kaukonen@helsinki.fi (A.M. Kaukonen).

1. Introduction

Many existing and new drug molecules (>95% of new potential therapeutics) suffer from poor pharmacokinetics [1], e.g., poor bioavailability when delivered orally. Contributing reasons to inadequate oral bioavailability are poor solubility and/or dissolution of the drug in the intestinal lumen, poor permeation properties in the gastrointestinal (GI) tract as well as high intestinal or hepatic first pass metabolism [2–4]. Hörter and Dressman suggest that compounds with aqueous solubilities lower than 100 $\mu\text{g/ml}$ are likely to show dissolution limited absorption [2]. However, the level of solubility required to minimize poor absorption

is dependent on the permeability and potency (dose) of a compound so that a poorly permeable compound would require a much higher solubility than, respectively, a highly permeable one [3]. Due to the present trends in drug discovery, delivery systems addressing issues related to crystal energy limited solubility and means to modulate drug permeability have been emphasized as key technologies [5].

Microfabricated porous materials offer a possibility to circumvent the above-mentioned dissolution related problems in oral drug delivery. The microparticles can be fabricated so that they are stable under the harsh conditions of the stomach and GI lumen maintaining their physicochemical properties unchanged, and function as non-erosive drug carriers/matrices [6]. The utilization of mesoporous microparticles to increase the solubility and the dissolution rate is based on the fact that the formation of crystalline material is restricted by the confined space of the pores, which are only a few times larger than the drug molecule, thus retaining the drug in its non-crystalline, disordered form [7]. The disordered or amorphous form is known to exhibit higher dissolution rates than its crystalline counterpart, especially when solubility is limited by high lattice energy [8,9]. The dissolution rate from porous materials will also be promoted by the high surface area (up to several hundreds of m²/g) characteristic of these carrier materials. Further benefits for improved dissolution are obtained through improved wetting properties of the particles [7]. Besides this, the potential of mesoporous materials to improve the permeability of biomolecules has been explored with insulin in combination with classical permeation enhancers [10], as well as the potential to provide controlled release for conventional drug molecules [11–15]. When functioning as controlled release carriers, nanosized mesoporous particles may serve as aids to enhance the circulatory persistence of drugs and to target drugs to specific cells [16].

Several studies have been published regarding the loading of drugs into mesoporous silica-based particles and the subsequent release behavior (e.g. [11–15,17,18]), but the potential of these particles to affect the permeation and/or absorption of the loaded drug has not been probed. In our previous study [7], the loading of furosemide in thermally carbonized mesoporous silicon microparticles (TCPSi) was found to enhance the release kinetics of furosemide and to reduce the pH dependence of the dissolution behavior. In the present study, the combined release and permeation of furosemide has been studied in order to assess the subsequent effects of improved dissolution from the TCPSi-loaded furosemide on the *in vitro* permeation across Caco-2 monolayers. Permeation was studied at apical pH-values of 5.5, 6.8 and 7.4, in order to address the potential of TCPSi-loading to improve absorption of furosemide via effects on dissolution and/or permeation of furosemide under conditions representative of upper and lower small intestinal contents. Furosemide dissolution rate and solubility is poor at low pH (5–20 µg/ml [19,20]), but increases steeply in a pH-dependent manner

so that furosemide has been classified as belonging to either BCS class IV or class III [21–23]. The relatively poor and variable oral absorption of furosemide (50–61% [24–27]), which occurs site-specifically in the stomach and upper small intestine [28,29], has been ascribed to the poor dissolution of furosemide at low pH [19] as well as the involvement of intestinal efflux proteins [30,31].

2. Materials and methods

2.1. Materials

Silicon wafers Si (100), of p+-type with resistivity values of 0.015–0.025 Ω cm, were used in the preparation of porous silicon (PSi). Furosemide was purchased from Sigma-Aldrich and used as received. Dulbecco's modified Eagle's medium (DMEM), non-essential amino acids (NEAA), heat-inactivated (+56 °C for 30 min) fetal bovine serum (FBS), L-glutamine (200 mM), antibiotic mixture (10,000 IU/ml penicillin G, 10,000 µg/ml streptomycin), Hanks' balanced salt solution (HBSS) and Hepes buffer solution (1 M) were from Gibco Invitrogen Corp. (Life Technologies Ltd., Paisley, Scotland) and 2-(*N*-morpholino)-ethanesulfonic acid (MES) from Sigma Chemical Co (St. Louis, MO, USA). D-[1-¹⁴C]mannitol (specific activity 59.0 mCi/mmol) was purchased from Amersham Pharmacia Biotech (England). Acetic acid was purchased from Riedel-de-Haën (Seelze, Germany), acetonitrile and methanol from Rathburn (Walkerburn, Scotland), phosphoric acid from Merck (Darmstadt, Germany). Water was purified in an Alpha-Q water-purification system (Millipore, Molsheim, France). Ethanol (ETAX Aa 99.5%) was purchased from Primalco (Helsinki, Finland). Dimethylsulfoxide (DMSO) used in drug loading was purchased from J.T. Baker B.V. (Holland).

2.2. Fabrication of drug-loaded porous microparticles

The preparation of drug-loaded porous microparticles was performed as described by Salonen et al. [7]. Shortly, the ball-milled free-standing porous silicon films were sieved several cycles with a 400 mesh sieve to obtain the desired particle size distribution. Prior to surface treatment by carbonization, the sieved microparticles were treated with HF:EtOH solution (1:1) to replace the oxidized surface formed, and the microparticles were filtered via a teflon membrane filter. A two-step thermal carbonization was used to stabilize the microparticles by the formation of SiC-terminated surface (thermally carbonized PSi; TCPSi).

Drug loading was performed at room temperature in a DMSO solution at 600 mg/ml furosemide as previously reported [7]. The microparticles were dried at a constant temperature (120 °C) oven until all solvent was removed. TG was used to determine residual solvent and the drying was continued until no traces of solvent could be found. Quantification of drug load was performed

immediately after the loading and is expressed as $w_{\text{drug}}/(w_{\text{drug}} + w_{\text{TCPSi}}) \times 100\%$.

2.3. Physical characterization of the microparticles

The samples were characterized utilizing thermogravimetry (TG; TGA 7, Perkin-Elmer, 10 °C/min, N₂ gas purge), differential scanning calorimetry (DSC; Pyris Diamond DSC, PerkinElmer, 2 °C/min, N₂ gas purge), helium pycnometry (AccuPyc 1330, Micromeritics) and N₂ ad/desorption studies (TriStar 3000, Micromeritics). FTIR studies were carried out using a Spectrum BX II (Perkin-Elmer) with a horizontal ATR accessory (MIRacle, Pike Technology, Inc.) at 4 cm⁻¹ resolution.

Details and rationale on the use of TG, DSC, He pycnometry and N₂ ad/desorption to determine drug loading have been reported previously [7,32,33]. The total drug load was also determined by HPLC from extracted samples according to Salonen et al. [7]. Extracted drug loads were used as a basis for calculation of %-released in the dissolution experiments.

2.4. Determination of furosemide ionization and partitioning constants

Ionization constants (pK_a) and octanol–water partitioning coefficients (log *P*) were determined using a computerized Sirius GLpKa-potentiometric titrator (firmware v.1.114, Sirius Analytical Instruments Ltd., Forest Row, UK) at controlled temperature (25 ± 1 °C) under argon flow. The results were processed using the Refinement Pro software. Blank titrations were performed at the start of each day to standardize electrode performance [34]. Apparent pK_a-values were determined in ionic strength adjusted methanol–water mixtures at several methanol concentrations and the aqueous pK_a-values obtained through the Yasuda–Shedlovsky extrapolation procedure. Partitioning coefficients of unionized (log *P*_{AH₂}) and mono-anionic (log *P*_{AH⁻}) furosemide were obtained from titrations in the presence of octanol using three different octanol–water volume ratios. The log *D* values were based on the determined log *P* values mentioned above and the log-linear dependence presented in Eq. (1) [21,35].

$$\log D_{\text{acid}} = \log P - \log(1 + 10^{\text{pH} - \text{pK}_a}) \quad (1)$$

2.5. Dissolution experiments

Dissolution experiments were performed as described earlier by Salonen et al. [7]. Experiments were performed in buffered (10 mM Hepes or MES) HBSS at pH 5.5, 6.8 and 7.4 utilizing Transwell cell culture inserts (polycarbonate membrane, pore size of 0.4 µm, 4.7 cm² area; Corning Costar Corp., Cambridge, MA, USA) and 6-well culture plates as donor and acceptor compartments, respectively.

All experiments were performed in triplicate and under sink conditions.

2.6. Caco-2 permeability experiments

2.6.1. Cell culture

The Caco-2 cells (ATCC, Rockville, MD, USA) were seeded at 6.8 × 10⁴ cells/cm² onto polycarbonate filter membranes (pore size 0.4 µm, growth area 1.1 cm²) in clusters of 12 wells (Transwell, Corning Costar Corp., Cambridge, MA, USA). The cells were grown in a medium consisting of DMEM (4.5 g/l glucose) supplemented with 10% FBS, 1% NEAA, 1% L-glutamine, penicillin (100 IU/ml), and streptomycin (100 µg/ml). The cultures were maintained at 37 °C (BB 16 gas incubator, Heraeus Instruments GmbH, Hanau, Germany) in an atmosphere of 5% CO₂ and 95% air, at 95% relative humidity. The growth medium was changed three times a week until time of use. Cells from passage numbers 31–42 were used in the experiments at ages ranging from 21 to 28 days.

2.6.2. Permeability experiments

The permeability of pre-dissolved furosemide (control solutions) or furosemide loaded into the TCPSi particles was studied across Caco-2 cell monolayers in an apical-to-basolateral (AP-BL) direction at an apical pH of 5.5, 6.8 (pH-gradient conditions) and 7.4 (iso-pH), and basolateral pH of 7.4. Control experiments of dispersed, unloaded furosemide were also performed under iso-pH conditions.

Before the permeability experiments, the cell monolayers were rinsed twice with HBSS, pH 7.4, and equilibrated in the transport buffers under experimental conditions for 30 min. Transepithelial electrical resistance (TEER) was measured using a Millicell[®] ERS Voltohmmeter (Millipore Corp., Bedford, MA, USA) and monolayers with TEER values below 250 Ω cm² were discarded. The mean TEER value at the start was 597 ± 68 Ω cm² across all monolayers used (*n* = 19). The apical solution was changed to HBSS containing furosemide or loaded TCPSi particles (1.0–1.5 mg per monolayer) (suspended immediately prior to experiments). Basolateral samples were obtained after 25, 50, 75, 100, 120, 150, and 180 min by moving the cell monolayers to a new receiver well containing fresh HBSS, pH 7.4. All of the transport experiments were conducted at least in triplicate (*n* = 3–4). Samples were kept at –22 °C until analysis (not longer than 5 days).

To determine monolayer integrity after each experiment, the cell cultures were washed once with HBSS at experimental pH, and the TEER values measured. Monolayer integrity was further assessed after the drug permeability tests with [¹⁴C]mannitol. The apical washing solution was changed to a test solution with [¹⁴C]mannitol solution (30 µl stock solution in 5 ml HBSS) at experimental pH conditions. After 60 min, 100 µl samples were withdrawn from the basolateral and apical compartments for activity measurements. Diffusion rates ≤ 0.5% per hour were taken as an indication of normal monolayer integrity.

2.7. Quantification of compounds

Analysis of furosemide concentrations was performed by HPLC (Waters Millennium, Milford, USA) using a Waters 470 Scanning Fluorescence Detector, a Waters 717 plus Autosampler, and a Waters 510 pump [7].

For determination of [^{14}C]mannitol, the 100 μl samples were mixed with 4 ml of a scintillation cocktail (Optiphase HiSafe 2, Wallac Fisher Chemicals, Loughborough, England), and [^{14}C]activities were determined using a WinSpectral 1414 Liquid Scintillation Counter (Wallac, Turku, Finland).

2.8. Data analysis

Cumulative amounts of drugs transported across Caco-2 cell monolayers were calculated from concentrations measured in the receiver (basolateral) compartments. Apparent permeability coefficients, P_{app} (cm/s), were calculated using Eq. (2)

$$P_{\text{app}} = \Delta Q / (\Delta t \cdot A \cdot C_0), \quad (2)$$

where $\Delta Q / \Delta t$ is the flux of compound across the monolayers ($\mu\text{g}/\text{min}$), A (cm^2) is the surface area of the cell monolayer, and C_0 is the initial concentration ($\mu\text{g}/\text{ml}$) of the compound in the donor (apical) compartment. Results reported are average P_{app} (cm/s) values \pm SD ($n = 3$ –4) based on data obtained up to 120 min. For TCPSi experiments, apparent permeability coefficients were estimated using C_0 values based on the complete dose contained in the TCPSi particles having dissolved. The dose was obtained from analysis of ethanol extracted samples ($n = 3$ –4) taken from the TCPSi suspension used in the permeation experiment.

Mass balance (recovery) was determined from the sum of the cumulative amount transported and residual drug in the donor compartment in relation to the initial amount in the donor compartment. To determine residual drug in TCPSi particles, the total volume of the donor compartment (0.5 ml) plus an additional wash with transport buffer (0.5 ml; to ensure complete removing of all TCPSi particles) were added into ethanol (1.0 ml), the sample filtered after 60 min of magnetic stirring, and the drug concentration analyzed by HPLC. Furosemide recovery in permeability experiments was $90 \pm 9\%$ ($n = 9$) and $90 \pm 13\%$ ($n = 10$) of initial drug in solution or contained in the TCPSi particles, respectively.

3. Results and discussion

3.1. Characteristics of TCPSi microparticles and loaded furosemide

The thermally carbonized porous silicon (TCPSi) microparticles provide a highly wettable, chemically inert/stable, mesoporous matrix with a high surface area ($248 \text{ m}^2/\text{g}$) suitable for drug loading [7]. The crystal form of furose-

mide (polymorph, solvate, amorphous) has been shown to depend greatly both on the used organic solvent and its water content as well as the method of precipitation [20,36]. In the case of TCPSi-loaded furosemide, the confined space of the pores (average pore size 12.1 nm) restricts the formation of crystalline material, the result of which was observed in the DSC measurements where neither the melting endotherm of bulk furosemide nor the melting endotherm of the small crystallites in the pores at reduced temperatures could be observed.

In addition to the HPLC assay of furosemide content (39.1%), loading into the TCPSi particles was quantified by TG (43%), He pycnometry (39.6%) and nitrogen sorption (41.2%), while DSC showed no traces of furosemide residing on the external surface of the porous particles [7]. The quantification of the drug load with TG required temperatures as high as 650 $^{\circ}\text{C}$. The thermogram of furosemide showed a sharp start of the decomposition at 234 $^{\circ}\text{C}$, after which faster decomposition followed (Fig. 1a). These different decomposition rates are clearly visible in derivated thermograms (Fig. 1b). The same rate

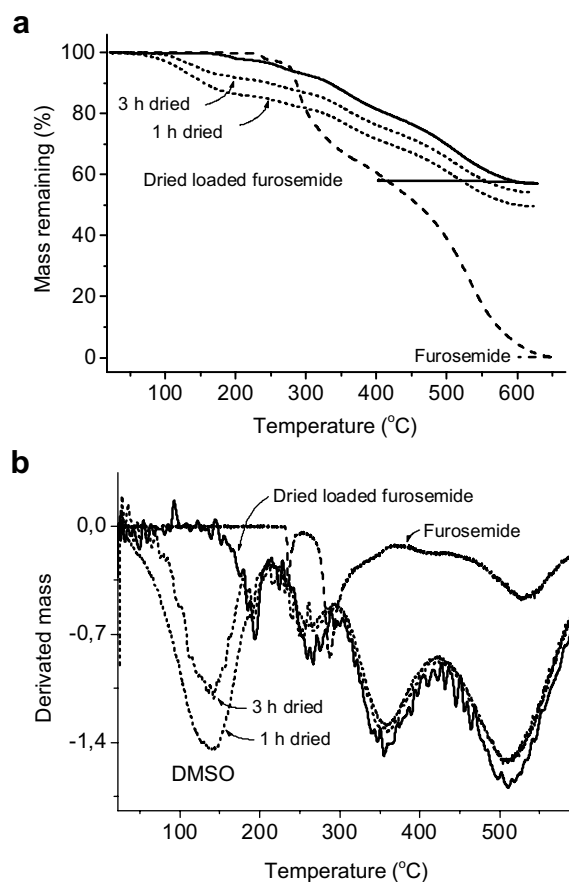


Fig. 1. (a) TG curves of unloaded (dashed) and loaded furosemide (solid), and two curves measured from samples during the drying process (short dashed). The heating rate was 10 $^{\circ}\text{C}/\text{min}$. (b) Derivated and smoothed TG curves showing clearly the negative additional peak arising from the DMSO desorption below 200 $^{\circ}\text{C}$.

variations could also be found in the loaded samples, although at slightly lower temperatures. In the samples measured during the drying process, a clear additional negative peak at temperatures below 200 °C could be seen. This is connected with desorption of DMSO and has been used in monitoring of the drying process. The drying process was continued until the peak arising from the DMSO desorption was absent.

Due to the slightly higher loading results obtained with the physical methods compared to the extracted samples analyzed by HPLC [7], questions were raised regarding potential chemical interactions between loaded drugs and the TCPSi microparticles. However, all the absorption peaks of furosemide were observed also in the FTIR spectra of the TCPSi-loaded furosemide while additional peaks were not observed (Fig. 2). This confirmed that furosemide was not bonded onto the microparticles through chemical interactions. In addition, no traces of the strong peaks of DMSO at 1042 and 1019 cm^{-1} could be found in the spectrum of the loaded microparticles indicating absence of DMSO after drying.

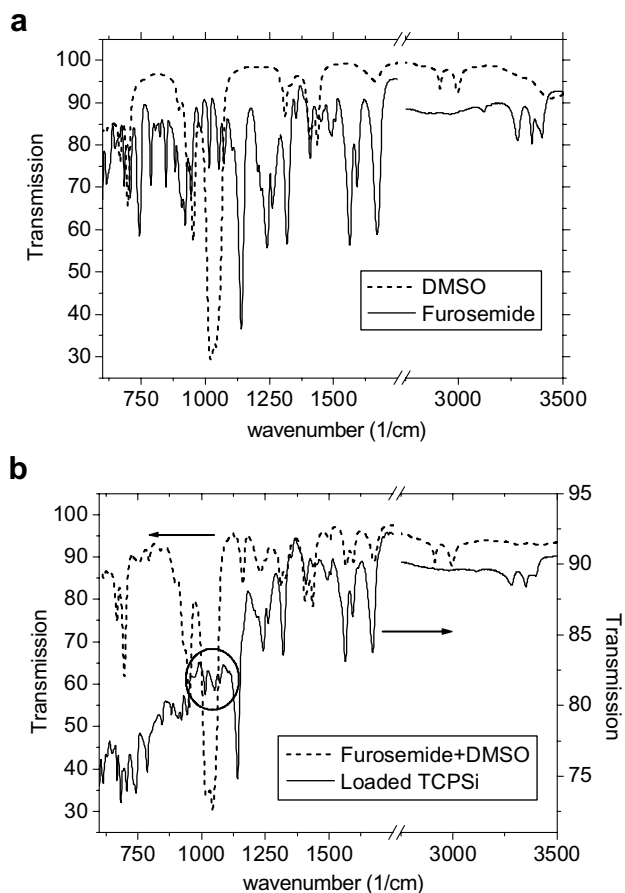


Fig. 2. FTIR spectra of DMSO (dashed) and furosemide (solid) alone (a) and in DMSO dissolved furosemide (dashed) and loaded microparticles (solid) (b). The circle in (b) indicates the area where the traces of DMSO should be the most visible.

3.2. Dissolution behavior of furosemide from TCPSi microparticles

Furosemide solubility is very pH sensitive [19–21] as is also demonstrated by the dissolution properties of unloaded furosemide presented in Fig. 3. However, as previously observed [7], the pH-dependence was remarkably reduced during dissolution from furosemide–TCPSi microparticles although release at pH 5.5 was still slightly slower than at pH 6.8 or 7.4. Nevertheless, dissolution from TCPSi particles was faster than that of unloaded furosemide across all pH-values studied, the effect being pronounced at pH 5.5.

Dissolution properties of furosemide have previously been found to depend on the crystal state and to increase especially in the case of an amorphous furosemide–PVP dispersion [19,20,36]. Similar to our results with the TCPSi-loaded furosemide, improved dissolution from the amorphous co-precipitate was observed especially at acidic pH and a super-saturation effect suggested. Interestingly, Doherty and York [19] were able to substantiate the differences observed *in vitro* in an *in vivo* study, where a more rapid onset of effect was observed from the PVP dispersion

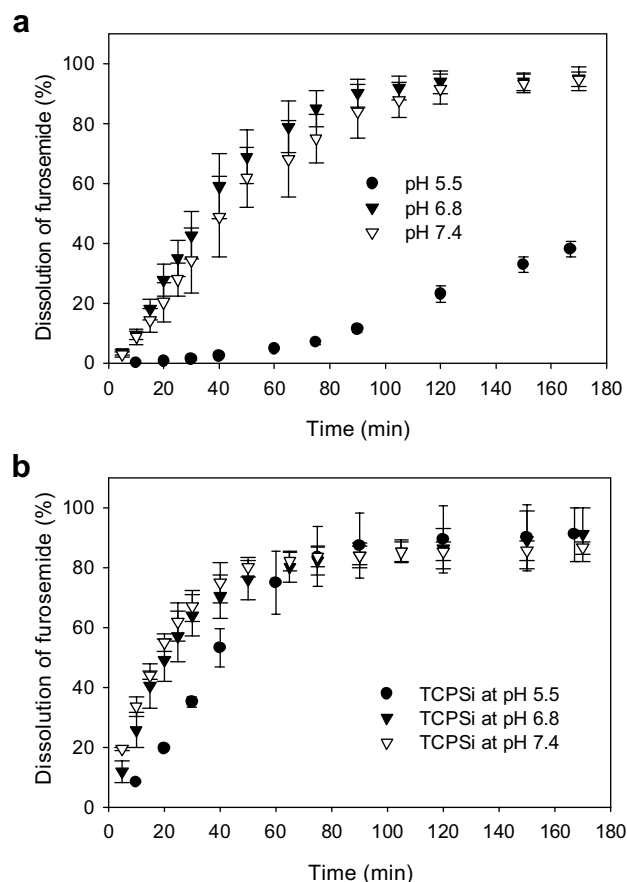


Fig. 3. Dissolution profiles (means \pm SD, $n = 3$) at pH 5.5 (●), 6.8 (▼) and 7.4 (▽) of (a) unloaded furosemide and (b) TCPSi-loaded furosemide.

containing amorphous furosemide compared to crystalline furosemide.

3.3. Integrity of Caco-2 monolayers during permeation experiments

The integrity of the Caco-2 monolayers was ensured prior to use in experiments by measuring the TEER-values after pre-equilibration in transport buffer. The resistance of the monolayers used was quite consistent, with a mean value of $597 \pm 68 \Omega \text{ cm}^2$ ($n = 19$) at the start of the experiment. The TEER values decreased in all experiments but did not drop below $250 \Omega \text{ cm}^2$ and the lowest value measured was $336 \Omega \text{ cm}^2$ after a pH 7.4 solution experiment (Table 1). Results on mannitol permeability performed after furosemide experiments gave consistently values below 0.5% per hour and further suggest that monolayer integrity was not compromised by the treatments.

3.4. Permeation of furosemide across Caco-2 monolayers

Furosemide permeation across Caco-2 monolayers was studied from pre-dissolved solutions (controls) and from furosemide containing TCPSi microparticles in the absorptive direction (apical-to-basolateral) utilizing apical pH conditions corresponding to the dissolution experiments and representative of the intestinal contents of the upper and lower small intestine. The concentration of the control solutions was intended to correspond to that obtained after dissolution of the dose contained in the TCPSi particles. However, at pH 5.5 the poor dissolution of furosemide precluded attainment of a sufficient concentration and a solution of $150 \mu\text{g/ml}$ was used. At pH 6.8 and 7.4 higher concentrations ($600 \mu\text{g/ml}$) were possible to attain, which provided a furosemide dose in control solution experiments that corresponded more closely to the dose contained in TCPSi microparticles. Due to the differences in drug content and concentration, also dose-corrected permeation profiles are presented in Fig. 4 (flux as % permeated) in order to provide more comparative data.

The highest permeability of pre-dissolved furosemide ($P_{\text{app}} 12.2 \pm 1.0 \times 10^{-6} \text{ cm/s}$) was observed when apical pH 5.5 was used, and the permeability decreased successively with increasing apical pH (Table 1). Furosemide is intrinsically a moderately lipophilic compound as demonstrated by the determined partitioning coefficients for

unionized furosemide ($\log P_{\text{AH}_2} 2.18 \pm 0.01$) and its mono-anion ($\log P_{\text{AH}^-} 0.02 \pm 0.07$). However, due to the high acid strength of furosemide (determined $\text{pK}_{\text{a}1} 3.70 \pm 0.04$, $\text{pK}_{\text{a}2} 9.93 \pm 0.09$), its lipophilicity decreases strongly across the studied pH range so that $\log D_{\text{pH}5.5}$ was estimated at 0.54 and $\log D_{\text{pH}7.4}$ at 0.03, respectively. In addition to the high ionization, the relatively high polar surface area of furosemide ($\text{PSA } 131 \text{ \AA}^2$, calculated using ACD/Labs pKa DB v.7.07, Advanced Chemistry Development Inc., Toronto, Canada) further contributes to a slow passive transcellular permeation of furosemide at higher pH values and it has been estimated that paracellular permeation represents a significant fraction of furosemide absorption at pH 7.4 [37,38]. Besides the favorable effect of lipophilicity, the relatively high permeability at pH 5.5 may be attributed to the presence of a pH gradient across the cell monolayer (basolateral chamber pH 7.4), which provides enhanced sink conditions through improved solubility properties at basolateral pH. Similar improvement in permeation has been observed upon addition of protein (BSA) to the receptor compartment, which has been ascribed to improved sink conditions provided by the high protein binding of furosemide [39].

Permeation profiles as μg - or %-permeated of TCPSi-loaded furosemide are presented in Fig. 4. Permeation of furosemide loaded into the TCPSi microparticles was higher than that obtained from corresponding solutions at each pH studied. As observed from Table 1, higher apparent permeation constants were obtained under all conditions, despite the fact that the P_{app} values for TCPSi-loaded furosemide were estimated assuming donor concentrations corresponding to total dissolution of furosemide contained in the TCPSi particles. Since dissolution of furosemide from particles would proceed simultaneously with permeation, the dose-based estimate overestimates the concentration and, hence, underestimates the P_{app} . However, the estimated P_{app} values are presented in order to demonstrate the improved permeability from the TCPSi particles.

Similar to the solution experiments, the overall highest permeability of furosemide from TCPSi microparticles ($P_{\text{app}} 18.0 \pm 1.3 \times 10^{-6} \text{ cm/s}$) was observed when apical pH 5.5 was used, which was 1.5-fold compared to that obtained with the pre-dissolved solution (Table 1). The observed flux (in $\mu\text{g/min}$) was in fact 5.2-fold to that obtained with the control solution (Fig. 4a), which is quite remarkable being the result of the combined dissolution

Table 1

Apparent permeabilities ($P_{\text{app}} \times 10^{-6} \text{ cm/s}$; means \pm SD, $n = 3-4$) of furosemide across Caco-2 monolayers from pre-dissolved furosemide (control solutions) and estimates for furosemide-loaded TCPSi microparticles

Apical pH	Control solutions			TCPSi microparticles ^a		
	Concn ($\mu\text{g/ml}$)	$P_{\text{app}} \times 10^{-6} \text{ (cm/s)}$	TEER (%)	Concn ($\mu\text{g/ml}$)	$P_{\text{app}} \times 10^{-6} \text{ (cm/s)}$	TEER (%)
pH 5.5	150	12.2 ± 1.0	95.1 ± 6.1	520	18.0 ± 1.3	82.0 ± 4.8
pH 6.8	600	0.93 ± 0.38	72.0 ± 0.9	840	4.1 ± 0.5	93.6 ± 4.7
pH 7.4	650	0.30 ± 0.01	76.8 ± 18.6	670	1.38 ± 0.05	88.0 ± 2.9

TEER-values after experiment are presented as % of initial (means \pm SD, $n = 3-4$).

^a P_{app} from TCPSi estimated using donor concentration based on completely dissolved furosemide dose in TCPSi microparticles.

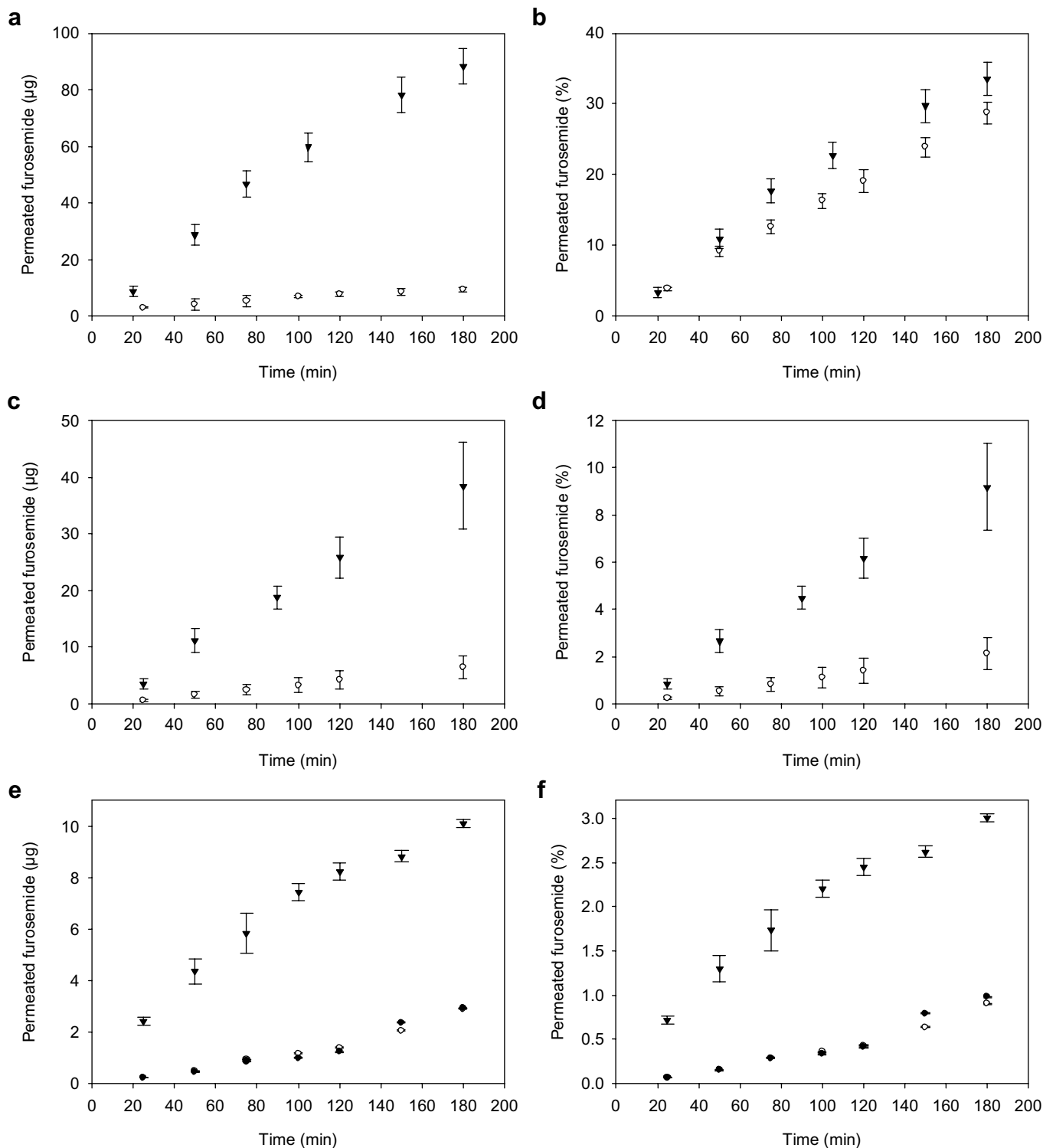


Fig. 4. Permeation of pre-dissolved (control) furosemide (empty circles), TCPSi-loaded furosemide (filled triangles) and suspended unloaded furosemide (filled circles) across Caco-2 monolayers (means \pm SD, $n = 3-4$) at apical pH 5.5 (frames a and b), pH 6.8 (c and d) and pH 7.4 (e and f). Frames a, c and e present results as amount (μg) and frames b, c and f as dose-corrected fraction of furosemide permeated as a function of time.

and permeation of a 3.5-fold dose compared to that in the pre-dissolved solution, especially considering the fact that the low solubility of furosemide was the reason behind the lower dose contained in the pre-dissolved solution.

At higher pH-values, where furosemide permeability from solutions decreased, the relative increase in P_{app} -values afforded by TCPSi-loading was correspondingly higher and a 4.7-fold increase in P_{app} -value was observed at apical pH

7.4, where the permeability of furosemide was the poorest (Fig. 4c and d). Interestingly, the permeation of suspended unloaded furosemide at pH 7.4 was lower than that of TCPSi-loaded and practically identical to that of pre-dissolved furosemide, in spite of the fact that the dissolution profile of unloaded furosemide at pH 7.4 does not differ remarkably from that of TCPSi-loaded furosemide (Fig. 3) [7]. Additional permeability experiments with pre-dissolved furosemide in the presence of unloaded TCPSi particles showed a slight increase in permeability (P_{app} -values 1.2-fold) suggesting modest effects on monolayer permeability of the TCPSi particles themselves (up to 120 min of exposure). These results indicate that increased paracellular permeability would not be the major component of the improved permeability of furosemide observed at higher pH values, which is also supported by the observed mannitol permeability and TEER values.

In addition to poor transcellular permeation properties, furosemide absorption may be hampered by active efflux transport, although it has not been explicitly established which efflux proteins are involved [30,31,37,40]. The secretory transport has been found saturable with a K_m -value of $63 \pm 28 \mu\text{M}$ [31], suggesting that the attainment of high local concentrations should increase the achieved net absorption. These studies were performed under iso-pH 7.4 to enable the investigation of polarized transport without the added effects of different ionization state and lipophilicity under different pH conditions. However, an acidic microclimate (pH range 5.2–6.2) exists at the enterocyte surface, maintained *in vivo* by the mucus layer and the secretion of H^+ -ions [21]. As the Caco-2 monolayers lack a distinct mucus layer (and hence a defined acidic microclimate region), results obtained using acidic apical media have provided more relevant information and a better correlation of permeation vs. fraction absorbed [26]. Hence, the scenario presented under acidic apical conditions could be considered more predictive of the *in vivo* situation especially considering that furosemide is mainly absorbed in the upper GI-tract [28,29], where also the acidic microclimate is pronounced [22,41].

4. Conclusions

In a previous study, furosemide was successfully loaded into porous silicon (PSi)-based microparticles, that had been thermally carbonized (TCPSi) to provide stable surface properties [7]. This presented furosemide with solid state properties more favorable to dissolution, and greatly diminished the pH dependence of dissolution. The present study showed that the improved dissolution was also translated into enhanced permeation from furosemide-loaded TCPSi particles across all pH conditions studied without any obvious effects on monolayer integrity. Permeability was enhanced especially at higher pH values where furosemide exhibits low permeability possibly due to the combined effects of high ionization and efflux mechanisms. However, the highest effects on the flux were observed at

lower pH values due to higher dosing potential afforded by the improved dissolution properties. Overall, the results suggest that the high local concentrations provided by the enhanced dissolution properties of TCPSi-loaded furosemide could prove beneficial for absorption.

Acknowledgements

The financial support from the Academy of Finland (Grant Nos. 211048 and 202258) and the National Technology Agency, Finland (Grant 40186/04), is acknowledged. The authors thank Erja Piitulainen for the HPLC determinations and Harri Nurmi for valuable assistance during pK_a and $\log P$ measurements.

References

- [1] D.J. Brayden, Controlled release technologies for drug delivery, *Drug Discov. Today* 8 (2003) 976–978.
- [2] D. Hörter, J.B. Dressman, Influence of physicochemical properties on dissolution of drugs in the gastrointestinal tract, *Adv. Drug Deliv. Rev.* 25 (1997) 3–14.
- [3] C.A. Lipinski, Drug-like properties and the causes of poor solubility and poor permeability, *J. Pharmacol. Toxicol. Method* 44 (2000) 235–249.
- [4] R. Panchagnula, N.S. Thomas, Biopharmaceutics and pharmacokinetics in drug research, *Int. J. Pharm.* 201 (2000) 131–150.
- [5] K.R. Horspool, C.A. Lipinsky, Advancing new drug delivery concepts to gain a lead, *Drug Deliv. Technol.* 3 (2002), 34, 36, 38, 40, 42, 44, 46.
- [6] J. Salonen, V.-P.B. Lehto, M.E. Laine, L. Niinistö, Chemical stability studies of thermally-carbonized porous silicon, *Mat. Res. Soc. (MRS) Symp. Proc.* 638 (2001), F14.19.1–6.
- [7] J. Salonen, L. Laitinen, A.M. Kaukonen, J. Tuura, M. Björkqvist, T. Heikkilä, K. Vaha-Heikkilä, J. Hirvonen, V.-P. Lehto, Mesoporous silicon microparticles for oral drug delivery: loading and release of five model drugs, *J. Control. Release* 108 (2005) 362–374.
- [8] L.-F. Huang, W.-Q.T. Tong, Impact of solid state properties on developability assessment of drug candidates, *Adv. Drug Deliv. Rev.* 56 (2004) 321–334.
- [9] L. Yu, Amorphous pharmaceutical solids: preparation, characterization and stabilization, *Adv. Drug Deliv. Rev.* 48 (2001) 27–42.
- [10] A.B. Foraker, R.J. Walczak, M.H. Cohen, T.A. Boiarski, C.F. Grove, P.W. Swaan, Microfabricated Porous Silicon Particles Enhance Paracellular Delivery of Insulin Across Intestinal Caco-2 Cell Monolayers, *Pharm. Res.* 20 (2003) 110–116.
- [11] J. Andersson, J. Rosenholm, S. Areva, M. Linden, Influences of material characteristics on ibuprofen drug loading and release profiles from ordered micro- and mesoporous silica matrices, *Chem. Mater.* 16 (2004) 4160–4167.
- [12] G. Cavallaro, P. Pierro, F.S. Palumbo, F. Testa, F. Luigim Pasqua, R. Aiello, Drug delivery devices based on mesoporous silicate, *Drug Delivery* 11 (2004) 41–46.
- [13] A.L. Doadrio, E.M.B. Sousa, J.C. Doadrio, J. Perez Pariente, I. Izquierdo-Barba, M. Vallet-Regi, Mesoporous SBA-15 HPLC evaluation for controlled gentamicin drug delivery, *J. Control. Release* 97 (2004) 125–132.
- [14] B. Munoz, A. Ramila, J. Perez-Pariente, I. Diaz, M. Vallet-Regi, MCM-41 organic modification as drug delivery rate regulator, *Chem. Mater.* 15 (2003) 500–503.
- [15] M. Vallet-Regi, J.C. Doadrio, A.L. Doadrio, I. Izquierdo-Barba, J. Perez-Pariente, Hexagonal ordered mesoporous material as a matrix for the controlled release of amoxicillin, *Solid State Ionics* 172 (2004) 435–439.
- [16] R. Aston, R. Saffie-Siebert, L. Canham, J. Ogden, Nanotechnology applications for drug delivery, *Pharm. Tech.* 17 (2005) 21–28.

- [17] C. Charnay, S. Begu, C. Tourne-Peteilh, L. Nicole, D.A. Lerner, J.M. Devoisselle, Inclusion of ibuprofen in mesoporous templated silica: drug loading and release property, *Eur. J. Pharm. Biopharm.* 57 (2004) 533–540.
- [18] C. Tourne-Peteilh, D. Brunel, S. Begu, B. Chiche, F. Fajula, D.A. Lerner, J.-M. Devoisselle, Synthesis and characterization of ibuprofen-anchored MCM-41 silica and silica gel, *New J. Chem.* 27 (2003) 1415–1418.
- [19] C. Doherty, P. York, The in-vitro pH-dissolution dependence and in-vivo bioavailability of frusemide–PVP solid dispersions, *J. Pharm. Pharmacol.* 41 (1989) 73–78.
- [20] Y. Matsuda, E. Tatsumi, Physicochemical characterization of furosemide modifications, *Int. J. Pharm.* 60 (1990) 11–26.
- [21] A. Avdeef, Physicochemical profiling (solubility, permeability and charge state), *Curr. Top. Med. Chem.* 1 (2001) 277–351.
- [22] A. Avdeef, *Absorption and Drug Development: Solubility, Permeability, and Charge State*, John Wiley and Sons Inc., Hoboken, 2003.
- [23] C.-Y. Wu, L.Z. Benet, Predicting drug disposition via application of BCS: transport/absorption/elimination interplay and development of a biopharmaceutics drug disposition classification system, *Pharm. Res.* 22 (2005) 11–23.
- [24] W.L. Chiou, H.Y. Jeong, S.M. Chung, T.C. Wu, Evaluation of using dog as an animal model to study the fraction of oral dose absorbed of 43 drugs in humans, *Pharm. Res.* 17 (2000) 135–140.
- [25] V. Pade, S. Stavchansky, Link between drug absorption solubility and permeability measurements in Caco-2 cells, *J. Pharm. Sci.* 87 (1998) 1604–1607.
- [26] S. Yamashita, T. Furubayashi, M. Kataoka, T. Sakane, H. Sezaki, H. Tokuda, Optimized conditions for prediction of intestinal drug permeability using Caco-2 cells, *Eur. J. Pharm. Sci.* 10 (2000) 195–204.
- [27] F. Ingels, B. Beck, M. Oth, P. Augustijns, Effect of simulated intestinal fluid on drug permeability estimation across Caco-2 monolayers, *Int. J. Pharm.* 274 (2004) 221–232.
- [28] E.A. Klausner, E. Lavy, D. Stepensky, E. Cserepes, M. Barta, M. Friedman, A. Hoffman, Furosemide pharmacokinetics and pharmacodynamics following gastroretentive dosage form administration to healthy volunteers, *J. Clin. Pharmacol.* 43 (2003) 711–720.
- [29] M. Säkkinen, T. Tuononen, H. Jurjenson, P. Veski, M. Marvola, Evaluation of microcrystalline chitosans for gastro-retentive drug delivery, *Eur. J. Pharm. Sci.* 19 (2003) 345–353.
- [30] S.D. Flanagan, L.Z. Benet, Net secretion of furosemide is subject to indomethacin inhibition, as observed in Caco-2 monolayers and excised rat jejunum, *Pharm. Res.* 16 (1999) 221–224.
- [31] S.D. Flanagan, C.L. Cummins, M. Susanto, X. Liu, L.H. Takahashi, L.Z. Benet, Comparison of furosemide and vinblastine secretion from cell lines overexpressing multidrug resistance protein (P-glycoprotein) and multidrug resistance-associated proteins (MRP1 and MRP2), *Pharmacology* 64 (2002) 126–134.
- [32] V.-P. Lehto, K.V. Heikkilä, J. Paski, J. Salonen, Use of thermoanalytical methods in quantification of drug load in mesoporous silicon microparticles, *J. Therm. Anal. Cal.* 80 (2005) 393–397.
- [33] J. Salonen, J. Paski, K. Vähä-Heikkilä, T. Heikkilä, M. Björkqvist, V.-P. Lehto, Determination of drug load in porous silicon microparticles by calorimetry, *Phys. Stat. Solid (A) Appl. Res.* 202 (2005) 1629–1633.
- [34] A. Avdeef, pH-metric log P. II: Refinement of partition coefficients and ionization constants of multiprotic substances, *J. Pharm. Sci.* 82 (1993) 190–193.
- [35] A. Leo, C. Hansch, D. Elkins, Partition coefficients and their uses, *Chem. Rev.* 71 (1971) 525–616.
- [36] C. Doherty, P. York, Frusemide crystal forms; solid state and physicochemical analyses, *Int. J. Pharm.* 47 (1988) 141–155.
- [37] S.D. Flanagan, L.H. Takahashi, X. Liu, L.Z. Benet, Contributions of saturable active secretion, passive transcellular, and paracellular diffusion to the overall transport of furosemide across adenocarcinoma (Caco-2) cells, *J. Pharm. Sci.* 91 (2002) 1169–1177.
- [38] V. Pade, S. Stavchansky, Estimation of the relative contribution of the transcellular and paracellular pathway to the transport of passively absorbed drugs in the Caco-2 cell culture model, *Pharm. Res.* 14 (1997) 1210–1215.
- [39] S.M. Chung, E.J. Park, S.M. Swanson, T.C. Wu, W.L. Chiou, Profound effect of plasma protein binding on the polarized transport of furosemide and verapamil in the Caco-2 model, *Pharm. Res.* 18 (2001) 544–547.
- [40] B.D. Rege, L.X. Yu, A.S. Hussain, James E. Polli, Effect of common excipients on Caco-2 transport of low-permeability drugs, *J. Pharm. Sci.* 90 (2001) 1776–1786.
- [41] Y.F. Shiao, P. Fernandez, M.J. Jackson, S. McMonagle, Mechanisms maintaining a low-pH microclimate in the intestine, *Am. J. Physiol. Gastrointest. Liver. Physiol.* 248 (1985) G608–G617.